Sustained wood burial in the Bengal Fan over the last 19 My

Hyejung Lee[a], Valier Galy[b], Xiaojuan Feng (冯晓娟)[c], Camilo Ponton[a,d], Albert Galy[e], Christian France-Lanord[e], and Sarah J. Feakins[a,1]

[a]Department of Earth Sciences, University of Southern California, Los Angeles, CA 90089; [b]Department of Marine Chemistry and Geochemistry, Woods Hole Oceanographic Institution, Woods Hole, MA 02543; [c]State Key Laboratory of Vegetation and Environmental Change, Institute of Botany, Chinese Academy of Sciences, 100093 Beijing, China; [d]Department of Geology, Western Washington University, Bellingham, WA 98225; and [e]Centre de Recherches Pétrographiques et Géochimiques, CNRS, Université de Lorraine, 54506 Vandoeuvre-lès-Nancy, France

Edited by Katherine H. Freeman, Pennsylvania State University, University Park, PA, and approved September 22, 2019 (received for review August 8, 2019)

The Ganges–Brahmaputra (G-B) River system transports over a billion tons of sediment every year from the Himalayan Mountains to the Bay of Bengal and has built the world's largest active sedimentary deposit, the Bengal Fan. High sedimentation rates drive exceptional organic matter preservation that represents a long-term sink for atmospheric CO_2. While much attention has been paid to organic-rich fine sediments, coarse sediments have generally been overlooked as a locus of organic carbon (OC) burial. However, International Ocean Discovery Program Expedition 354 recently discovered abundant woody debris (millimeter- to centimeter-sized fragments) preserved within the coarse sediment layers of turbidite beds recovered from 6 marine drill sites along a transect across the Bengal Fan (~8°N, ~3,700-m water depth) with recovery spanning 19 My. Analysis of bulk wood and lignin finds mostly lowland origins of wood delivered episodically. In the last 5 My, export included C_4 plants, implying that coarse woody, lowland export continued after C_4 grassland expansion, albeit in reduced amounts. Substantial export of coarse woody debris in the last 1 My included one wood-rich deposit (~0.05 Ma) that encompassed coniferous wood transported from the headwaters. In coarse layers, we found on average 0.16 weight % OC, which is half the typical biospheric OC content of sediments exported by the modern G-B Rivers. Wood burial estimates are hampered by poor drilling recovery of sands. However, high-magnitude, low-frequency wood export events are shown to be a key mechanism for C burial in turbidites.

carbon cycle | wood | lignin | Himalaya | Bengal Fan

The burial of terrestrial biospheric organic carbon (OC) in marine sediments represents a net transfer of carbon from the atmosphere to the sedimentary reservoir, where it may be stored over geologic timescales, thereby decreasing CO_2 and increasing O_2 levels in the atmosphere (1, 2). Fine-grained sediments containing phyllosilicates with high surface area have high OC content and can shield OC from degradation through mineral interactions (3). As such, the supply and accumulation of clay minerals has been considered to be key to the preservation of both marine and terrestrial OC in marine sediments (4, 5) while coarse sediments and OC particles have received little attention (6, 7).

Coarse plant debris has recently been found to be a significant component of the OC load in small mountainous rivers with high erosion rates and brief sediment transit times (8–11). If coarse wood is efficiently supplied to and preserved in marine sediments (6, 7, 12), the burial of coarse (>1 mm) OC particles may thus play an important—yet overlooked—role in the sequestration of atmospheric CO_2. Here, we investigate the sourcing, transport, and burial of coarse woody debris in the largest active sedimentary system on Earth, the Bengal Fan.

International Ocean Discovery Program (IODP) Expedition 354 drilled 7 sites on a west–east transect at 8°N in the middle Bengal Fan, *ca*. 2,000 km away from the mouth of the rivers that currently supply sediments (*SI Appendix*, Fig. S1). We sampled cores from 3 deep sites that provide a record of sedimentation history over the last 19 My (*SI Appendix*, Fig. S2), 3 shorter records to sample sediments of the last 1 My, and excluded another, site U1449, on the basis of high deposition rates (13). Wood was visually identified and removed from split cores onboard the *R/V Joides Resolution* and further recovery was achieved in postexpedition research by sieving millimeter- to centimeter-scale wood from the sediment matrix (detailed in *Materials and Methods*).

We analyzed the molecular and isotopic composition of the woody debris (detailed in *Materials and Methods*) to reveal information about sourcing within the catchment based on environmental gradients (e.g., elevation, C_3/C_4 vegetation, and precipitation). We explore the implications of composition to reveal transport and preservation/degradation mechanisms of the overlooked woody component of fluvially exported terrestrial carbon. Given the size of the Ganges–Brahmaputra (G-B) catchment (1.6×10^6 km^2) and the Bengal Fan (3×10^6 km^2), and the long distance of sediment transport (>2,000 km offshore), the frequent presence of wood fragments is remarkable. Although clay minerals have been considered to be the predominant means for the preservation of terrestrial OC in marine sediments, evidence for wood burial in these coarse turbiditic

Significance

The Bengal Fan is the largest sedimentary deposit in the world and has previously been shown to represent a major sink of carbon that may have contributed to the Cenozoic cooling trend. Wood transport has been observed in rivers during the high flows of the monsoon season, or associated with events such as cyclones, earthquake-triggered landslide and dam-and-release events from the mountains. However, wood was not widely thought to survive export and burial in the oceans. This study shows that woody debris can survive thousands of kilometers of transport in rivers and in turbidites, to be deposited in the fan. Wood has been overlooked in quantification of organic carbon burial on continental margins.

Author contributions: H.L., V.G., C.P., A.G., C.F.-L., and S.J.F. designed research; H.L., V.G., X.F., C.P., A.G., C.F.-L., and S.J.F. performed research; H.L., V.G., X.F., C.F.-L., and S.J.F. analyzed data; and H.L., V.G., and S.J.F. wrote the paper.

The authors declare no competing interest.

This article is a PNAS Direct Submission.

Data deposition: Datasets reported in this paper are also available via the National Oceanic and Atmospheric Administration Paleoclimatology database (https://www.ncdc.noaa.gov/paleo-search/study/27770).

[1]To whom correspondence may be addressed. Email: feakins@usc.edu.

This article contains supporting information online at www.pnas.org/lookup/suppl/doi:10.1073/pnas.1913714116/-/DCSupplemental.

First published October 21, 2019.

sediments means that similar units merit attention when assessing OC burial in other marginal settings.

Wood Burial in the Bengal Fan

Turbidites dominate the sedimentary accumulation of the Bengal Fan and millimeter- to centimeter-sized wood debris was picked from the coarse-grained layers of turbidites beds, especially subunits Tb and Td of the Bouma sequence (14) during visual description of the split cores onboard the *R/V Joides Resolution* (Fig. 1). Wood was mainly found as 1) isolated large fragments within thick sandy deposits, 2) small fragments dispersed throughout the coarse basal units of turbidite layers and, 3) (sub) horizontal layers of fragments concentrated at the transition between coarse and fine sediments (i.e., the subunit Td of the Bouma sequence). The wood fragments varied in color and size but were most commonly gray or black in color, in thin sheets (likely as a result of compaction and dewatering) or small amorphous fragments. Bigger pieces (up to 3 cm × 2 cm) were mostly brown to black, but some layers yielded abundant and apparently unaltered (pale-colored) wood fragments.

Our survey of woody horizons spanned 19 My of sediments (Fig. 2), and in total 60 coarse horizons yielded visible wood (up to ∼6 g) that was picked from the core surface (Fig. 2*A*). In order to further survey for cryptic occurrences of wood, we sieved (>1 mm) 73 additional coarse horizons across the 19 My. We recovered wood debris from 37 out of 73 sieved samples, with up to 4.21 g of wood or 8.64 weight % (hereafter %) of sediment (Fig. 2*A*). In total, we recovered up to ∼6 g wood per 1 My (Fig. 2*B*), with 97 wood samples spanning the last 19 My (Fig. 2*C*). We found wood at each of the drill sites that we studied (U1450, U1451, U1452, U1453, U1454, and U1455). The age–depth distribution of samples reveals the episodic deposition of woody horizons and the extent of our core sampling coverage (Fig. 2*D*), including overlapping sediment recovery, that attempted to account for spatial variations in deposits as the channel–levee complexes migrate. However, we emphasize neither the coring, nor our sampling of the cores, allows for comprehensive accounting of all wood buried at this location. A critical obstacle is that coarse sediments have the lowest sediment recoveries (*SI Appendix*, Fig. S2), and thus wood-bearing horizons have been disproportionately missed in drilling. In addition, thousands of coarse horizons were recovered—many of which contain wood debris based on visual inspection of core section photographs—and we did not sample all of them. Nevertheless, we captured evidence of wood deposits throughout the last 19 My.

All 97 wood-bearing turbidites were sampled in triplicate to determine the C concentration of wood fragments (in weight %, hereafter %). We found wood C concentration ranging from 3.89 to 81.43% (mean = 33.49%, 1σ =14.02%, n = 257; Dataset S3). The mean is close to that expected for living wood, typically 40 to 55% C (15). Low C concentration (<40%) may result from degradation processes or dilution by silicate mineral matrix embedded within wood fragments. Three samples with 80% C likely represent charred wood. We find no systematic trend in wood C content over the 19-My record, suggesting limited degradation of wood debris following burial.

Normalizing for the mass of sediment, we found that wood concentration was 0.31 ± 1.13% (1σ, n = 70), and wood C

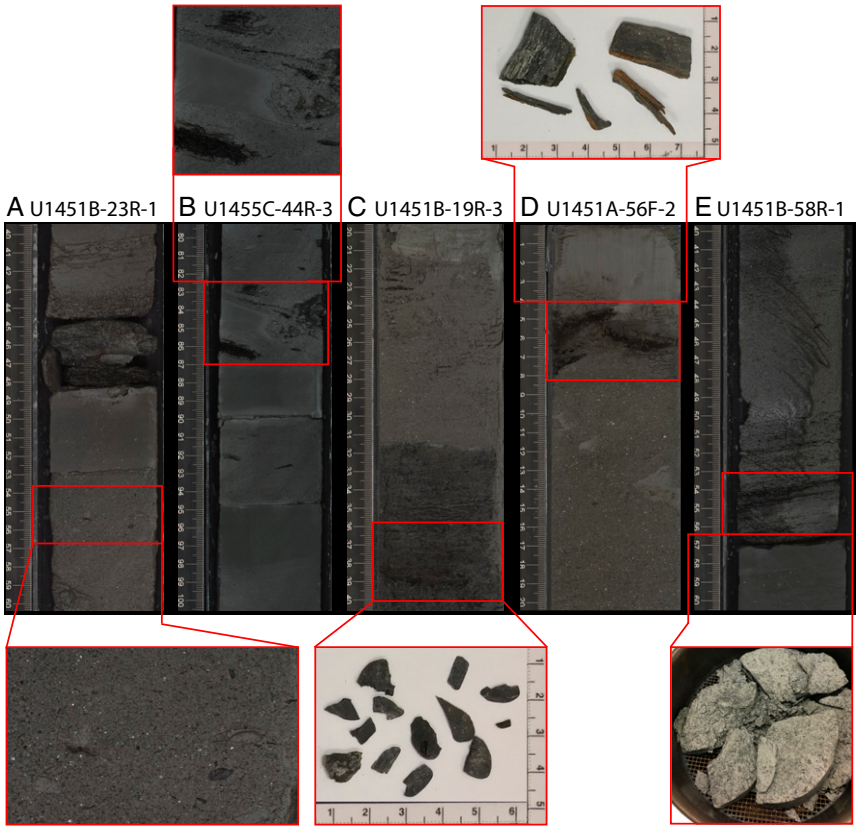

Fig. 1. Five examples of wood deposits in IODP Expedition 354 cores from sites U1451 and U1455. Buried wood sizes vary from millimeter- to centimeter-scale and are denoted by black fragments on core images (IODP LIMS Reports). Samples with readily visible wood pieces such as in (*A*) U1451B-23R-1 (47 to 49 cm, red box), (*B*) U1455C-44R-3 (85 to 87 cm), and (*D*) U1451A-56F-2 (4 to 7 cm) were picked directly from the face of the split cores. Other layers with visible specks, thought to be wood, were sieved to isolate fragments, including samples of (C) U1451B-19R-3 (36 to 40 cm) and (*E*) U1451B-58R-1 (50 to 56 cm). All rulers show centimeters.

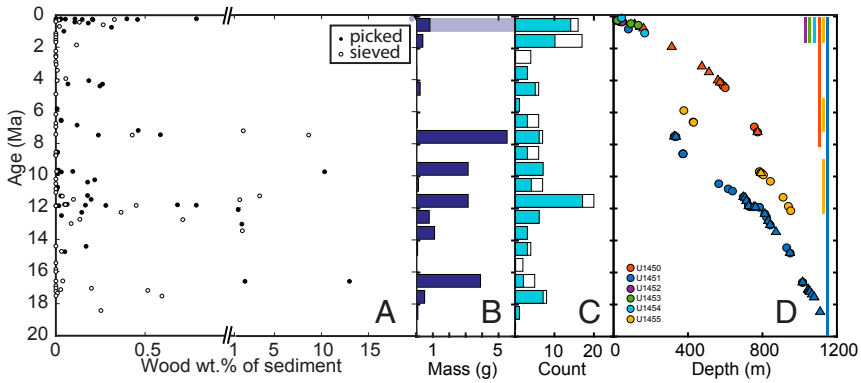

Fig. 2. Semiquantitative accounting of wood abundance. (*A*) Wood mass normalized to sediment mass including picked (solid) and sieved samples (open symbols). (*B*) Wood mass summed in 1-My bins (dark blue). One high-abundance picked sample at 0.05 Ma, highlighted in light purple in *A* and *B*, is estimated >5 g. (*C*) Count of wood-yielding samples (cyan) and total samples (white). (*D*) The age–depth distribution of wood fragments compared to the sampled span of cores to the right. Age estimates for sample depths are provided in Dataset S1 with explanation in *Materials and Methods*. Note core recovery is discontinuous and sedimentation rates vary (*SI Appendix*, Fig. S2). For wood mass per sample by core site see *SI Appendix*, Fig. S3.

concentration was 0.15 ± 0.43% (1σ, n = 34) for the sieved samples (Dataset S3). For the picked samples, the sediment mass relating to core surface sampling was not well constrained. We hence assign an average mass of sediment (30 g) in order to estimate concentrations of wood, at 0.94 ± 3.27% (1σ, n = 60) and wood C as 0.17 ± 0.62% (1σ, n = 59) of sediment mass. This assumption suggests that sieved samples had on average lower wood mass recovery than the picked samples, which is reasonable as the picked samples targeted large fragments and/or high abundance horizons, with visibly apparent wood on the split core surface. Across all of the studied coarse horizons, we find that wood mass is 0.60 ± 2.39% (n = 130) of sediment mass and wood C is 0.16 ± 0.55% (n = 93) of sediment mass. These OC concentrations are higher than that of the coarse load of the modern G-B Rivers (typically *ca*. 0.05%), where OC is almost entirely petrogenic (16). This observation requires the addition of wood fragments, above the OC concentrations observed over the last few decades in the G-B Rivers, and this likely occurs during extreme sediment export events in rivers. The addition of wood to the coarse sediment load is significant with respect to the carbon cycle. Indeed, wood photosynthetic C represents a net carbon sequestration mechanism, whereas the background petrogenic C present in coarse river sediments is only being transferred from terrestrial to marine long-term storage (with potential for loss in transit). As such, wood-laden coarse sediment transport and deposition becomes an effective carbon sequestration mechanism.

Although large wood debris has been analyzed in rivers (9, 10, 17–19), there are only a few studies of wood export to the ocean (11, 20) and even fewer investigating wood preservation and burial in marine turbidites (6, 7, 12). Intense physical erosion events such as landslides may export wood to the oceans in small mountainous rivers. For example, Typhoon Morakot triggered landslides in Taiwan in August 2009 delivering ∼3.8 to 8.4 Tg of coarse woody debris to the oceans, representing 30 to 60% of the river-exported terrestrial biospheric carbon (21). The resulting turbidites (7) further transported the wood offshore where it was buried with up to 70% preservation efficiency (6), which is attributed in part to the short distances in small mountain rivers (22). In the very large G-B catchment (1.6×10^6 km^2), extreme erosion events and associated sediment transport have been observed in the high-relief regions of the modern system and/or documented in the geological record, during earthquake, landslide, and glacial-dam outburst floods (23–27). Although some events originate above the tree line, land sliding also occurs within forested zones and high-flow conditions entrain coarse woody debris downstream. In such high-discharge events, wood erosion may follow the "pulse–shunt" concept proposed for dissolved OC (28), with a pulse of input and a shunt of increased velocity, leading to efficient carbon export. However, we are aware of no prior studies that have tried to quantify wood export fluxes to the oceans from large mountainous river catchments. Infrequent, high-flow export events are challenging to capture both in modern river systems and in ancient fan deposits where the locus of deposition shifts over time.

Our sampling of the transect of IODP Expedition 354 cores, focused on locating visible wood fragments within the coarse turbidites to establish the abundance and characteristics of such deposits. Given the length of the G-B Rivers and the >2,000-km distance from the river mouth to deposition, the presence of wood in deep sea sediments of the mid Bengal Fan throughout the last 19 My demonstrates wood export and burial efficiency. Our discovery of wood distributed throughout the 19-My record indicates the need to account for buried wood in carbon budgets by surveying carbon throughout turbidites in order to quantify the contribution of wood to the long-term (10^7-y) sequestration of atmospheric CO_2. However, accurate accounting of such fluxes is challenging as the locus of deposition changes as the canyon–levee systems migrate across the fan (29) and low recovery of coarse-grained sediments during drilling (*SI Appendix*, Fig. S2) may lead to underestimates of wood burial.

Galy et al. (16) documented a negative relationship between grain size and OC content in the G-B sediments. Using this relationship, Acoustic Doppler Current Profiler to achieve depth integrations of sediment composition and flux, and ^{14}C-based estimates of petrogenic C content, they estimated the average biospheric OC concentration of suspended sediments exported by the Lower Meghna River (the confluence of the Ganges and Brahmaputra Rivers) to be 0.30% (30). We estimate that coarse-grained sediments deposited in the Bengal Fan contain half as much biospheric OC as the average G-B River suspended sediment and thus wood should be considered in global C burial budgets and petroleum source rock characterization. However, further partitioning of the relative importance of OC burial flux in fine and coarse sediments is not possible for several reasons. First, in river studies, coarse-grained fluvial export is less well studied than the fine particulate load. Second, in marine cores, the low recovery of sands compared to high recovery of clay-rich sediments, biases attempts at overall quantification. Third, IODP Expedition 354 drill sites sit along a 300-km transect orthogonal to the main direction of sediment delivery in efforts to capture the migrating channels supplying turbiditic sediments to the

fan (13). However, we do not yet have a view of transport of wood from the subaerial delta to the fan's terminal lobes (across 3×10^6 km^2), as would be needed to obtain a comprehensive budget of the overall burial of woody debris. Nevertheless, the results of IODP Expedition 354 show that coarse sediments represent a large proportion of the overall sediment deposition in the distal Bengal Fan (13). Combined with our observations of frequent wood debris preservation in coarse sediments, we demonstrate that the contribution of wood debris to the overall burial of terrestrial biospheric OC is significant.

Wood Composition Reveals Sourcing

Next, we studied the chemical structure and isotopic composition of buried wood in order to understand its ecological and geographic origin (Fig. 3). Lignin, a large heterogeneous aromatic polymer and the second-most-abundant biochemical in vascular plants, carries information about wood type and degradation in its phenolic structures (31). A subset of wood horizons ($n = 15$) were analyzed for lignin phenol composition across the 19-My record, with multiple analyses ($n = 9$) possible from one abundant horizon at 0.05 Ma (*Materials and Methods*). The relative abundance of syringyl (S) versus vanillyl (V) phenols indicated that almost all wood fragments were derived from angiosperms (S/V > 0.02) across the 19-My record (31, 32) (Fig. 3*A*). As angiosperms dominate below 2,500 m elevation in the G-B catchment, and conifers dominate above 3,000 m (33), phenolic composition constrains the elevation source to below 2,500 m. Predominantly lowland provenance has previously been documented for fine particulates in the modern G-B River system for bulk OC (16) and vascular plant biomarkers (34). Similarly, a persistent lowland provenance was inferred for OC associated with fine-grained sediments deposited in the Bengal Fan over the last 20 ky (35). Only in the Pleistocene, at ~0.05 Ma, did we find gymnosperm wood (S/V = 0.0), for 6 of 9 aliquots of a single horizon (Fig. 3*A* and Dataset S2), representing a distal, high-Himalayan origin. This may reflect a rare mass wasting event such as may occur with earthquakes, floods, or glacier retreat in high-relief mountain areas. For example glacial-lake outburst failures (23, 24) have been shown to move high sediment loads and large boulders tens of kilometers downstream. However, no modern observations have shown scenarios in which Himalayan coarse OC can be exported rapidly to the Bay of Bengal, as is required to explain the deposit we have documented at 0.05 Ma.

In addition to visual observations of compaction and color change in the fragments of wood, lignin phenol analysis indicates progressive degradation in wood fragments from 6 to 18 Ma (Miocene). With increasing age, we found declining concentrations of S, V and *p*-hydroxyl (P) phenols and increasing acid-to-aldehyde ratios for the S and V groups (Sd/Sl and Vd/Vl, respectively; *SI Appendix*, Fig. S4), indicative of degradation (36). As S phenols are preferentially lost compared to V phenols during wood degradation, the directional trend in S/V over the Miocene is ascribed to progressive degradation (Fig. 3). However, lignin degradation is not extensive as both Sd/Sl (mean = 0.32, 1σ = 0.15, $n = 23$) and Vd/Vl (mean = 0.37, 1σ = 0.15, $n = 23$) fall largely within the range (<0.4) expected for fresh wood (15).

Stable carbon isotopic composition was measured to identify variations in source wood as may result from altitude, humidity, and use of the C_3 versus C_4 photosynthetic pathway. Bulk wood $\delta^{13}C$ ($\delta^{13}C_{wood}$) values range from −30.4 to −11.4‰ in 97 turbidites (each horizon sampled in triplicate, yielding 257 individual measurements spanning the last 19 My; Fig. 3*B*). We find no correlation between wood C content and $\delta^{13}C_{wood}$ (*SI Appendix*, Fig. S5 and *SI Extended Supplementary Data Discussion*), which implies that degradation and/or matrix dilution does not systematically affect $\delta^{13}C_{wood}$. From 18.4 to 5.8 Ma, we find that $\delta^{13}C_{wood}$ values in discrete turbiditic horizons range between −29.9 and −23.8‰ (mean = −26.6‰, 1σ = 1.2‰, $n = 187$). Aliquots within a single horizon have an average variability of 0.7‰ (1σ) that represents heterogeneity within a single coarse-grained horizon of the turbiditic deposit, which could readily derive from variations within a localized plant community (e.g., species differences or microhabitat). The 6.1‰ range between turbidites suggests deposits retain the character of input events (floods, cyclones, etc.) with varied sourcing within the large catchment. This further suggests minimal mixing during fluvial and submarine transport to the edge of the shelf and during resuspension in turbiditic transport to the midfan core location. The apparent stationarity of the range of $\delta^{13}C_{wood}$ values from 18.4 to 5.8 Ma implies no systematic change in climate, ecosystem, or sourcing across this 12-My period of the Miocene (Fig. 3*B* and *SI Appendix*, *SI Extended Supplementary Data Discussion*). After a gap in wood recovery from 5.8 to 4.42 Ma, a systematic shift begins at 4.42 Ma,

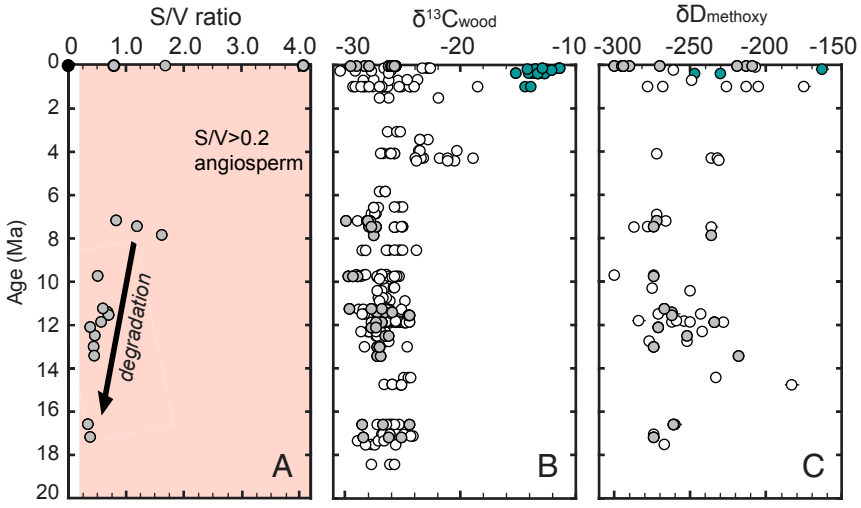

Fig. 3. Isotopic composition and phenol ratio of wood fragments in the Bengal Fan. (*A*) Syringyl/vanillyl, where S/V > 0.2 (gray circle) are angiosperms and arrow indicates degradation. One horizon at 0.05 Ma contains the only gymnosperms (black circle, 6 overlying datapoints). (*B*) Bulk wood $\delta^{13}C$ and (*C*) lignin methoxy δD. Samples with phenol measurements (gray); C_4 plants (blue circle). Isotopic data differentiated by IODP site in *SI Appendix*, Fig. S3).

with a $\delta^{13}C_{wood}$ measurement of −20.5‰, which is 3.3‰ more positive than the most ^{13}C-enriched sample during the Miocene, which may suggest a mixture of C_3 and C_4 fragments within the aliquot. Even more ^{13}C-enriched values appear in the last 1 My, where $\delta^{13}C_{wood}$ values are bimodal with a C_4-like cluster (mean = −13.1‰, σ = 1.0‰, n = 17) as well as the typical C_3-like values (mean = −26.3‰, σ = 1.7‰, n = 51). This suggests a change in the ecosystems from which the wood is being exported (e.g., plant type and climate), with one-third of the buried wood derived from C_4 plants in the last 1 My.

As bulk tree wood is infrequently reported in modern ecosystems, we report $\delta^{13}C_{wood}$ from a survey of the woody tissues of trees, bamboo-like grass, and ferns collected along 2 elevation transects in Arunachal Pradesh (India) and Nepal within the G-B catchment in 2004 to 2007 (Dataset S4) and find that modern wood $\delta^{13}C$ values range from −23.1 to −33.2‰. We account for the year of sampling to remove the Suess effect and determine preindustrial equivalent values ($\delta^{13}C_{pre\text{-}I}$) relative to an atmospheric $\delta^{13}C_{atm}$ value of −6.4‰ (37). $\delta^{13}C_{pre\text{-}I}$ range from −21.4 to −31.4‰ with an average of −26.8‰, similar to buried wood samples from 18.4 to 5.8 Ma. We find no systematic difference between plant type (gymnosperm, angiosperm tree or shrub, bamboo, or fern) but we do observe an overall tendency to ^{13}C-enrichment with elevation of +0.8‰ km^{-1} (r^2 = 0.22, P < 0.001, n = 53; *SI Appendix*, Fig. S6) within C_3 plants. Much more enriched values are associated with the use of the C_4 pathway: One tall grass collected at 1,500 m yielded a $\delta^{13}C$ value of −12.7‰; another was collected in the lowlands, from the bank of the Ganges, where C_4 are dominant (−12.4‰; preindustrial equivalent −10.6‰).

C_4 Expansion in the G-B Catchment and Wood Sourcing

In the late Miocene (after ∼6.5 Ma) there was an ecosystem transformation associated with a C_4 grassland expansion detected in the Siwalik Formation in the Himalayan foreland (38, 39) and in bulk OC and biomarkers in the fine sediments of the Bengal Fan (40, 41). This region was the center of radiation in the C_4 Andropogoneae subfamily (42). Today the catchment includes many tall C_4 grasses (*Miscanthus*, *Saccharum*, *Hyparrhenia*, and *Heteropogon*), with stems that include woody tissues that may be strong enough to survive fluvial transport. Although expansion of the C_4 pathway is most commonly associated with grasslands (monocots), the C_4 pathway also appeared in some dicotyledenous plants (dicots), mostly shrubs that occupy ephemeral streams and saline habitats (43, 44) and Euphorbiaceae trees (43, 45). Only in glacial periods with lowered pCO_2 and drier conditions in the region may C_4 dicots have a competitive advantage over other plants (44). Pollen from the Siwalik Formation indicate the Miocene appearance of xeric and halophilic shrubs (*Amaranthaceae* and *Chenopodaceae*) (39). Those taxa are also represented along with Euphorbiaceae pollen in the last 1 My in the distal Bengal Fan, south of Sri Lanka (46). However, the C_4 pathway is most prevalent within tropical grasses in the catchment today, and tall grasses are therefore also assumed to be the most likely source of C_4 "wood" delivered in the last 5 My. Whether grass, shrub, or tree, C_4 plants generally grow below elevations of 1,500 m and thus add to the evidence for lowland sourcing of woody debris found in the Bengal Fan.

After the C_4 expansion we find signs of reduced burial of woody material in the Bengal Fan, based on barren horizons between 5.8 and 4.42 Ma (Fig. 2*A*). The grasslands that transformed ecosystems across the floodplains may have altered fluvial geomorphology and erosive processes (e.g., via changing rooting structures and plant lifecycle). Alternatively, this gap may reflect a shift in fan sedimentation processes as channel–levee deposition increases around this time (47).

During glacial cycles of the last 1 My, wood deposits have a bimodal $\delta^{13}C$ distribution likely reflecting wet, closed lowland forest and C_4 grass/xeric taxa at interglacial and glacial extremes, respectively (46, 48). Enhanced physical erosion likely explains the observed increase in wood export in the last 1 My, and this included export of C_4 with some aliquots yielding $\delta^{13}C$ values characteristic of pure C_4 plants (mean −13.0‰, σ = 1.0‰, n = 17) between 0.4 and 0.1 Ma. We hypothesize that these fragments were mainly deposited during glacial periods when aridity and low pCO_2 favored C_4 plants in lowland part of the G-B catchment (35). Supporting evidence comes from Pleistocene pollen in Deep Sea Drilling Project site 717 which were dominated by Gramineae (grass) pollen (presumably C_4), with enhanced transport of *Pinus* pollen from Himalayan sources in cold intervals (46). The buried wood record from the Bengal Fan indicates that C_4 woody debris is at times very abundant in the Pleistocene and provides catchment-scale evidence for the timing and magnitude of their expansion. Very low $\delta^{13}C_{wood}$ values are also observed during the Pleistocene, suggesting wood transport and burial was also effective for wet, closed forest wood, perhaps growing during interglacial periods. The Pleistocene stands out as an interval of extreme variability in wood composition that reflects cyclical climate variability and the resulting changes in vegetation and erosion as conditions change, including one instance of high-elevation sourcing, in contrast to dominantly lowland sourcing throughout the long record.

Constraints on the Isotopic Composition of Precipitation

We additionally sought constraints on isotopes in precipitation from the buried wood samples. The methoxy groups on lignin have the advantage of nonexchangeable hydrogen (unlike bulk wood, cellulose, or lignin) such that their hydrogen isotopic composition ($\delta D_{methoxy}$) records the isotopic composition of precipitation (δD_{precip}). A global survey of modern trees reported the fractionation ($^2\varepsilon_{methoxy/precip}$) between δD_{precip} and $\delta D_{methoxy}$ to be −216 ± 17‰ (1σ, n = 222) (49, 50). We measured buried wood samples from the Bengal Fan spanning 19 My, finding $\delta D_{methoxy}$ values range from −300 to −150‰ (mean = −253‰, 1σ = 30.5‰, n = 59; Fig. 3*C*). Applying the global fractionation, we estimated δD_{precip} values from the buried wood samples to range from −108 to +68‰ (mean = −48‰, σ = 39‰, n = 59; Dataset S6).

Modern δD_{precip} in the catchment ranges from −81 to −28‰ (amount-weighted mean annual precipitation from 25 sites all situated below 2,000 m; *SI Appendix*, Fig. S6 and Dataset S5). Most buried wood δD_{precip} estimates overlap with the range of modern precipitation range in the catchment and this suggests broadly comparable monsoonal precipitation patterns during the last 19 My. A few samples are slightly more D-depleted and suggest a high elevation source (>2,000 m) or a period of intensified monsoonal rainfall (51, 52) compared to the modern data. The power of dual-isotope analyses to diagnose altitude of sourcing has previously been demonstrated for plant wax biomarkers in another large, very wet tropical montane catchment, where both ^{13}C enrichment and D depletion are expected with increasing elevation (53). Here we extend that concept to buried wood measuring $\delta^{13}C_{wood}$ and $\delta D_{methoxy}$. Accordingly, samples with $\delta D_{methoxy}$ values below −280‰ and $\delta^{13}C_{wood}$ > −26.0‰ (Fig. 4) potentially derived from high altitude. However, overall the wood compositional distribution is not dominated by the expected altitude trends in each isotope system (*SI Appendix*, Figs. S6 and S7), indicating other factors contribute to the variability, in particular C_4 inputs, compositional variability within the lowland G-B catchment, and uncertain fractionation factors.

Three horizons have elevated $\delta D_{methoxy}$ (>200‰), and while we calculate δD_{precip} of +42 to +68‰ for these horizons, such enriched values are unlikely from meteoric water or evaporated surface waters. Instead, we suspect smaller fractionation factors

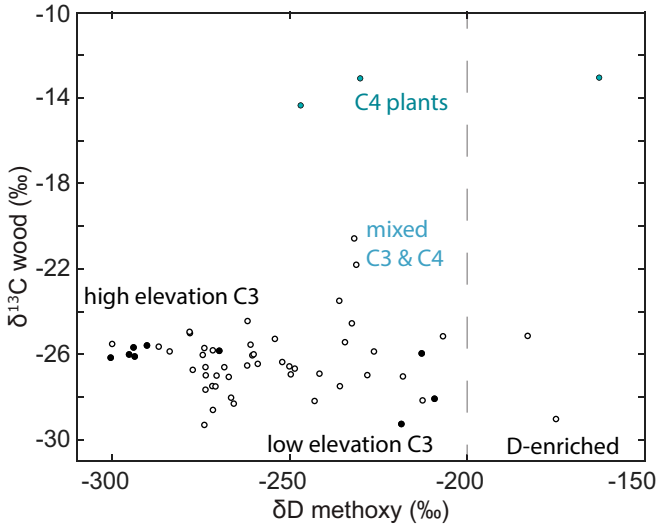

Fig. 4. Comparison of $\delta D_{methoxy}$ and $\delta^{13}C_{wood}$ for paired analyses on individual horizons (open symbols). The 0.05-Ma horizon (black symbols) was parsed into 9 aliquots of which 6 appear to be upland-derived based on dual isotopes (consistent with lignin evidence that they are gymnosperm) and 3 lowland-derived (consistent with their angiosperm identification); see *Discussion*. Annotations show expected altitudinal pattern within C_3 plants, ^{13}C-enrichment with mixed and pure C_4 horizons (blue symbols, $n = 3$ horizons), and anomalously D-enriched values (right of dashed line).

may be appropriate for those plants, and we note that the buried wood dataset includes C_4 plants which have not yet been calibrated for $^{2}\varepsilon_{methoxy/precip}$. Combining information from carbon and hydrogen isotope systems can also help to diagnose any such complications associated with C_4 inputs (Fig. 4). C_4 plant-derived wood samples are clearly differentiated by carbon isotopes and overall carry more D-enriched values typical of more lowland sources, although some yield values that are anomalously high. However, several C_3 plants are unexpectedly D-enriched as well, suggesting a need for local calibration of $\delta D_{methoxy}$ among C_3 as well as C_4 plants.

One abundant deposit, at 0.05 Ma, included large fragments that allowed for multiple aliquots for multiple analyses representing individual trees. In that sample, 6 fragments yielded lignin phenolic evidence for gymnosperms (conifers), thus derived from elevations above 2,500 m. Dual isotopes confirm that interpretation (Fig. 4). In those gymnosperm fragments we measured $\delta D_{methoxy}$ (mean = −291‰, 1σ = 14‰, n = 6) yielding δD_{precip} estimates of −95‰, independently corroborating a high-elevation provenance. In the same samples $\delta^{13}C$ values (mean = −25.9‰, 1σ = 0.2‰, $n = 6$) also support a high-elevation source. In contrast, 3 angiosperm fragments from this same horizon yield high δD_{precip} estimates (mean = +3‰, σ = 6‰, $n = 3$) and $\delta^{13}C$ values (mean = −27.8‰, 1σ = 1.7‰, $n = 3$) indicative of lowland sourcing (Fig. 4), suggesting mixing in transit. As discussed previously, there are several possible mechanisms to explain high-elevation sourcing including earthquake-triggered landslides or glacial damming, either of which can trigger lake outburst flooding with sediment loads and velocities well above normal monsoon flood conditions. Such an event could mobilize a large amount of woody debris from a high-elevation "point source" that can be transported rapidly to lower elevations, entraining wood from the lowlands, and perhaps triggering hyperpycnal flow facilitating rapid delivery to the deep sea. Although such events are reported in the Himalaya, and described offshore of small mountain rivers, a Himalaya-to-Bengal Fan transport event has not been observed in the modern system that is heavily altered with damming, channelization, and agriculture.

Conclusions

Geochemical analyses of wood preserved in the Bengal Fan show that remarkably well-preserved, lowland angiosperm wood dominates the largest size fraction of the wood recovered. Although most woody horizons carry the hallmarks of lowland sources, we find one unusual horizon at 0.05 Ma that indicates catastrophic erosion processes carrying gymnosperms from high altitude to the mid-Bengal Fan. Throughout the record, the range of $\delta^{13}C_{wood}$ and $\delta D_{methoxy}$ within and between sedimentary horizons indicates heterogeneous sources within the lowland part of the catchment. Although the Miocene climate, vegetation, and wood-erosive regime appears relatively stable from this wood-derived record, we see a major transition with $\delta^{13}C$ evidence for an increase in woody C_4 vegetation in the catchment (represented in the wood record after 4.42 Ma) and further expansion in the glacial phases of the Pleistocene (last 1 Ma). The wood horizons of the Pleistocene stand out against the 19-My record as a time of heightened variability in source characteristics.

OC burial in the Bengal Fan has been shown to be 4 to 5 times more efficient in sequestering atmospheric CO_2 than Himalayan silicate weathering and has therefore been proposed as one of the forcing factors of Cenozoic cooling (1, 54). The discovery of woody fragments in the coarse-grain layers of turbidite beds across 19 My indicates that woody input may be a neglected contributor to the OC cycle in the Bengal Fan and in other continental margins over geologic timescales. This has potential implications not only for OC burial budgets that have previously underestimated the OC content of continental margin sands (55, 56) but also for the fossil fuel generation potential of coarse siliciclastic sediments (12). The rapid export and burial of wood represents a highly efficient pathway of atmospheric CO_2 sequestration. Large-magnitude, low-frequency rapid wood transport bypasses degradation that can occur in soils, where extensive OC degradation limits the efficiency of OC burial at very high erosion rates (54). If triggered by high-discharge events, wood erosion may follow the "pulse–shunt" concept proposed for dissolved OC (28) with high flow pushing wood swiftly through rivers allowing for high OC burial efficiency under enhanced physical erosion rates.

Materials and Methods

Study Site. IODP Expedition 354 drilled 7 sites across a 320-km transect at 8°N in the mid Bengal Fan (mean water depth 3,650 m, deepest sediment recovery 1,200 m below the sea floor). Middle to Late Pleistocene ages were modeled using an approach that factors litho-, magneto-, bio-, cyclo-, and seismic stratigraphic constraints, based on results from the IODP Expedition 354 Bengal Fan and analysis of the GeoB97-020/027 seismic line (57).

Isolation of Wood from the Sediment Core. Sampling targeted wood-bearing coarse-grained horizons. Wood fragments were visually identified and picked from the split core face using stainless-steel tweezers (58 samples). Similar coarse-grain turbidites were sampled, freeze-dried, disassociated, and sieved (>1 mm) to retrieve wood fragments (73 samples). In this manner, we retrieved wood from marine sediments spanning 19 My.

Isotopic Analyses. For bulk wood OC and $\delta^{13}C$ analyses, 50 to 150 μg powdered wood was treated with 4% HCl at 85 °C for 1 h to remove carbonate, before measurement by elemental analyzer isotope ratio mass spectrometry. OC is reported in percent on a mass basis. $\delta^{13}C$ values are reported relative to the Vienna Pee Dee Belemnite/Lithium carbonate standard by L. Svec isotopic scale, with precision and accuracy better than 0.3‰. Wood fragments were not homogenized prior to taking aliquots, and thus triplicate measurements inform on compositional variability, with each sample containing a variable number of wood fragments depending on their size (1 large to >100 small pieces). For lignin methoxy hydrogen isotopic analyses, 20 to 80 mg of powdered wood was reacted with HI to release CH_3I then dissolved into isooctane for analysis by gas chromatography isotope ratio mass spectrometry, following the methods of ref. 58. Data are reported on the Vienna Standard Mean Ocean Water/Standard Light Antarctic Precipitation isotopic scale, with precision and accuracy better than 6‰. Due to the

size requirement, no replicates were possible except from one abundant coarse sample at 0.05 Ma where each measurement represents a single fragment.

Lignin Analyses. Ground wood was transferred into Teflon-lined bombs for CuO oxidation to isolate lignin-derived phenols. The wood was reacted with 0.5 g CuO, 100 mg ammonium iron (II) sulfate hexahydrate, and 3 mL of 12 M sodium hydroxide (NaOH) under N_2 at 170 °C for 2.5 h. After the reaction, the water phase was acidified to pH 1 with 6 M HCl and kept for 1 h at room temperature in the dark to prevent reactions of cinnamic acids. After centrifugation (2,500 rpm for 30 min), the supernatants were liquid–liquid-extracted with diethyl ether. The ether extracts were concentrated by rotary evaporation, spiked with a known amount of internal standard (ethyl vanillin), transferred to 2-mL glass vials, and dried under N_2 for gas chromatography mass spectrometry analysis.

Data Availability. All data have been publicly archived in the National Oceanic and Atmospheric Administration Paleoclimate database (59).

ACKNOWLEDGMENTS. This work was funded by National Science Foundation Grants OCE-1401217 and COL-T354A55 to S.J.F. and OCE-1400805 to V.G. Graduate student participation in the project received support from University of Southern California Provost's Fellowship to H.L. Samples were provided by the International Ocean Discovery Program. We are grateful for the efforts of the Expedition 354 Science Party, Carl Johnson, and Zongguang Liu. C.F.-L. and A.G. were supported by IODP-France. We thank Colin Osborne and Maria Vorontsova for helpful discussions.

1. C. France-Lanord, L. A. Derry, Organic carbon burial forcing of the carbon cycle from Himalayan erosion. *Nature* **390**, 65–67 (1997).
2. J. M. Hayes, J. R. Waldbauer, The carbon cycle and associated redox processes through time. *Philos. Trans. R. Soc. Lond. B Biol. Sci.* **361**, 931–950 (2006).
3. L. M. Mayer, Surface area control of organic carbon accumulation in continental shelf sediments. *Geochim. Cosmochim. Acta* **58**, 1271–1284 (1994).
4. J. I. Hedges, R. G. Keil, Sedimentary organic-matter preservation–An assessment and speculative synthesis. *Mar. Chem.* **49**, 81–115 (1995).
5. M. J. Kennedy, T. Wagner, Clay mineral continental amplifier for marine carbon sequestration in a greenhouse ocean. *Proc. Natl. Acad. Sci. U.S.A.* **108**, 9776–9781 (2011).
6. S. J. Kao *et al*., Preservation of terrestrial organic carbon in marine sediments offshore taiwan: Mountain building and atmospheric carbon dioxide sequestration. *Earth Surf. Dynam.* **2**, 127–139 (2014).
7. R. B. Sparkes *et al*., Redistribution of multi-phase particulate organic carbon in a marine shelf and canyon system during an exceptional river flood: Effects of Typhoon Morakot on the Gaoping River–Canyon system. *Mar. Geol.* **363**, 191–201 (2015).
8. A. G. West, G. R. Goldsmith, I. Matimati, T. E. Dawson, Spectral analysis software improves confidence in plant and soil water stable isotope analyses performed by isotope ratio infrared spectroscopy (IRIS). *Rapid Commun. Mass Spectrom.* **25**, 2268–2274 (2011).
9. J. I. Seo, F. Nakamura, D. Nakano, H. Ichiyanagi, K. W. Chun, Factors controlling the fluvial export of large woody debris, and its contribution to organic carbon budgets at watershed scales. *Water Resour. Res.* **44**, W04428 (2008).
10. J. M. Turowski, R. G. Hilton, R. Sparkes, Decadal carbon discharge by a mountain stream is dominated by coarse organic matter. *Geology* **44**, 27–30 (2016).
11. N. Kramer, E. Wohl, B. Hess-Homeier, S. Leisz, The pulse of driftwood export from a very large forested river basin over multiple time scales, Slave River, Canada. *Water Resour. Res.* **53**, 1928–1947 (2017).
12. A. Saller, R. Lin, J. Dunham, Leaves in turbidite sands: The main source of oil and gas in the deep-water Kutei Basin, Indonesia. *AAPG Bull.* **90**, 1585–1608 (2006).
13. C. France-Lanord *et al*., "Expedition 354 summary" in *Proceedings of the Ocean Drilling Program* (Integrated Ocean Drilling Program, College Station, TX, 2016), **vol 354**, pp. 1–35.
14. A. H. Bouma, P. H. Kuenen, F. P. Shepard, *Sedimentology of Some Flysch Deposits: A Graphic Approach to Facies Interpretation* (Elsevier, Amsterdam, 1962), pp. 168.
15. S. C. Thomas, A. R. Martin, Carbon content of tree tissues: A synthesis. *Forests* **3**, 332–352 (2012).
16. V. Galy, C. France-Lanord, B. Lartiges, Loading and fate of particulate organic carbon from the Himalaya to the Ganga-Brahmaputra delta. *Geochim. Cosmochim. Acta* **72**, 1767–1787 (2008).
17. R. G. Hilton, A. Galy, N. Hovius, M.-J. Horng, H. Chen, The isotopic composition of particulate organic carbon in mountain rivers of Taiwan. *Geochim. Cosmochim. Acta* **74**, 3164–3181 (2010).
18. E. Wohl, Bridging the gaps: An overview of wood across time and space in diverse rivers. *Geomorphology* **279**, 3–26 (2017).
19. A. M. Gurnell, H. Piégay, F. Swanson, S. Gregory, Large wood and fluvial processes. *Freshwater Biol.* **47**, 601–619 (2002).
20. E. L. Leithold, R. S. Hope, Deposition and modification of a flood layer on the northern California shelf: Lessons from and about the fate of terrestrial particulate organic carbon. *Mar. Geol.* **154**, 183–195 (1999).
21. A. J. West *et al*., Mobilization and transport of coarse woody debris to the oceans triggered by an extreme tropical storm. *Limnol. Oceanogr.* **56**, 77–85 (2011).
22. E. L. Leithold, N. E. Blair, K. W. Wegmann, Source-to-sink sedimentary systems and global carbon burial: A river runs through it. *Earth Sci. Rev.* **153**, 30–42 (2016).
23. K. L. Cook, C. Andermann, F. Gimbert, B. R. Adhikari, N. Hovius, Glacial lake outburst floods as drivers of fluvial erosion in the Himalaya. *Science* **362**, 53–57 (2018).
24. S.-Y. Huang *et al*., Late Pleistocene sedimentary history of multiple glacially dammed lake episodes along the Yarlung-Tsangpo river, southeast Tibet. *Quat. Res.* **82**, 430–440 (2014).
25. D. R. Montgomery *et al*., Evidence for holocene megafloods down the tsangpo river gorge, southeastern tibet. *Quat. Res.* **62**, 201–207 (2004).
26. D. A. Cenderelli, E. E. Wohl, Peak discharge estimates of glacial-lake outburst floods and "normal" climatic floods in the Mount Everest region, Nepal. *Geomorphology* **40**, 57–90 (2001).
27. R. A. Mir, S. K. Jain, A. K. Lohani, A. K. Saraf, Glacier recession and glacial lake outburst flood studies in Zanskar basin, western Himalaya. *J. Hydrol.* **564**, 376–396 (2018).
28. P. A. Raymond, J. E. Saiers, W. V. Sobczak, Hydrological and biogeochemical controls on watershed dissolved organic matter transport: Pulse-shunt concept. *Ecology* **97**, 5–16 (2016).
29. M. E. Weber, M. Wiedicke-Hombach, H. R. Kudrass, H. Erlenkeuser, Bengal Fan sediment transport activity and response to climate forcing inferred from sediment physical properties. *Sediment. Geol.* **155**, 361–381 (2003).
30. V. Galy, C. Hein, C. France-Lanord, T. I. Eglinton, "The evolution of carbon signatures carried by the Ganges-Brahmaputra river system: A source-to-sink perspective" in *Biogeochemical Dynamics at Major River-Coastal Interfaces: Linkages with Global Change*, M. A. Allison, T. S. Bianchi, W.-J. Cai, Eds. (Cambridge University Press, Cambridge, 2013), pp. 353–372.
31. J. I. Hedges, D. C. Mann, The characterization of plant tissues by their lignin oxidation products. *Geochim. Cosmochim. Acta* **43**, 1803–1807 (1979).
32. M. Winterfeld, M. A. Goñi, J. Just, J. Hefter, G. Mollenhauer, Characterization of particulate organic matter in the Lena River delta and adjacent nearshore zone, NE Siberia–Part 2: Lignin-derived phenol compositions. *Biogeosciences* **12**, 2261–2283 (2015).
33. C. Carpenter, The environmental control of plant species density on a Himalayan elevation gradient. *J. Biogeogr.* **32**, 999–1018 (2005).
34. V. Galy, T. Eglinton, C. France-Lanord, S. Sylva, The provenance of vegetation and environmental signatures encoded in vascular plant biomarkers carried by the Ganges-Brahmaputra rivers. *Earth Planet. Sci. Lett.* **304**, 1–12 (2011).
35. C. J. Hein *et al*., Post-glacial climate forcing of surface processes in the Ganges–Brahmaputra river basin and implications for carbon sequestration. *Earth Planet. Sci. Lett.* **478**, 89–101 (2017).
36. J. I. Hedges, G. L. Cowie, J. R. Ertel, R. J. Barbour, P. G. Hatcher, Degradation of carbohydrates and lignins in buried woods. *Geochim. Cosmochim. Acta* **49**, 701–711 (1985).
37. H. Friedli, H. Lotscher, H. Oeschger, U. Siegenthaler, B. Stauffer, Ice core record of the $^{13}C/^{12}C$ ratio of atmospheric CO_2 in the past 2 centuries. *Nature* **324**, 237–238 (1986).
38. J. Quade, J. M. L. Cater, T. P. Ojha, J. Adam, T. Mark Harrison, Late Miocene environmental change in Nepal and the northern Indian subcontinent: Stable isotopic evidence from paleosols. *Geol. Soc. Am. Bull.* **107**, 1381–1397 (1995).
39. C. Hoorn, T. Ohja, J. Quade, Palynological evidence for vegetation development and climatic change in the Sub-Himalayan Zone (Neogene, Central Nepal). *Palaeogeogr. Palaeoclimatol. Palaeoecol.* **163**, 133–161 (2000).
40. C. France-Lanord, L. A. Derry, $\delta^{13}C$ of organic carbon in the Bengal Fan: Source evolution and transport of C_3 and C_4 plant carbon to marine sediments. *Geochim. Cosmochim. Acta* **58**, 4809–4814 (1994).
41. K. H. Freeman, L. A. Colarusso, Molecular and isotopic records of C_4 grassland expansion in the late Miocene. *Geochim. Cosmochim. Acta* **65**, 1439–1454 (2001).
42. C. P. Osborne, Atmosphere, ecology and evolution: What drove the Miocene expansion of C_4 grasslands? *J. Ecol.* **96**, 35–45 (2008).
43. R. F. Sage, J. R. Coleman, Effects of low atmospheric CO_2 on plants: More than a thing of the past. *Trends Plant Sci.* **6**, 18–24 (2001).
44. J. R. Ehleringer, T. E. Cerling, B. R. Helliker, C_4 photosynthesis, atmospheric CO_2, and climate. *Oecologia* **112**, 285–299 (1997).
45. R. F. Sage, Environmental and evolutionary preconditions for the origin and diversification of the C4 photosynthetic syndrome. *Plant Biol.* **3**, 202–213 (2001).
46. Y. Yasuda, K. Amano, T. Yamanoi, "Pleistocene climatic changes as deduced from a pollen analysis of Site 717 cores" in *Proceedings of the Ocean Drilling Program* (Integrated Ocean Drilling Program, College Station, TX, 1990) vol. 116, chap. 21, pp. 249–257.
47. T. Schwenk, V. Spiess, "Architecture and stratigraphy of the bengal fan as response to tectonic and climate revealed from high-resolution seismic data" in *External Controls on Deep-Water Depositional Systems*, B. Kneller, O. J. Martinsen, B. McCaffrey, Eds. (Society for Sedimentary Geology, Tulsa, OK, 2009), vol 92, pp. 107–131.
48. E. Van Campo, Monsoon fluctuations in two 20,000-yr BP oxygen-isotope/pollen records off southwest India. *Quat. Res.* **26**, 376–388 (1986).
49. T. Anhäuser, M. Greule, D. Polag, G. J. Bowen, F. Keppler, Mean annual temperatures of mid-latitude regions derived from δ^2H values of wood lignin methoxyl groups and its implications for paleoclimate studies. *Sci. Total Environ.* **574**, 1276–1282 (2017).
50. F. Keppler *et al*., Stable hydrogen isotope ratios of lignin methoxyl groups as a paleoclimate proxy and constraint of the geographical origin of wood. *New Phytol.* **176**, 600–609 (2007).
51. C. N. Garzione, J. Quade, P. Decelles, N. English, Predicting paleoelevation of Tibet and the Himalaya from δ18 O vs. altitude gradients in meteoric water across the Nepal Himalaya. *Earth Planet. Sci. Lett.* **183**, 215–229 (2000).

52. A. P. Gajurel, C. France-Lanord, P. Huyghe, C. Guilmette, D. Gurung, C and O isotope compositions of modern fresh-water mollusc shells and river waters from the Himalaya and Ganga plain. *Chem. Geol.* **233**, 156–183 (2006).
53. S. J. Feakins, M. S. Wu, C. Ponton, V. Galy, A. J. West, Dual isotope evidence for sedimentary integration of plant wax biomarkers across an Andes-Amazon elevation transect. *Geochim. Cosmochim. Acta* **242**, 64–81 (2018).
54. V. Galy, B. Peucker-Ehrenbrink, T. Eglinton, Global carbon export from the terrestrial biosphere controlled by erosion. *Nature* **521**, 204–207 (2015).
55. D. J. Burdige, Preservation of organic matter in marine sediments: Controls, mechanisms, and an imbalance in sediment organic carbon budgets? *Chem. Rev.* **107**, 467–485 (2007).
56. D. J. Burdige, Burial of terrestrial organic matter in marine sediments: A re-assessment. *Glob. Biogeochem. Cycle* **19**, GB4011 (2005).
57. B. T. Reilly, "Deciphering quaternary geomagnetic, glacial, and depositional histories using paleomagnetism in tandem with other chronostratigraphic and sedimentological approaches", PhD thesis, Oregon State University, Corvallis (2018).
58. H. Lee, X. Feng, M. Mastalerz, S. J. Feakins, Characterizing lignin: Combining lignin phenol, methoxy quantification, and dual stable carbon and hydrogen isotopic techniques. *Org. Geochem.* **136**, 103894 (2019).
59. H. Lee *et al*., Bengal Fan 19 million year buried wood fragment data. NOAA Paleoclimate Database. https://www.ncdc.noaa.gov/paleo/study/27770. Deposited 24 September 2019.